Microwave and Optical Technology Letters

RESEARCH ARTICLE

Stable Dual-Beam Metasurface Antenna Array Based on Wideband Positive Phase Response Method

Peidong Feng | Lihan Wang | Jiangtao Zhang | Jianbo Sun | Xianglu Tang | Xiangchuan Wang | Shilong Pan

National Key Laboratory of Microwave Photonics, Nanjing University of Aeronautics and Astronautics, Nanjing, Jiangsu, China

Correspondence: Lihan Wang (andwwlh@nuaa.edu.cn)

Received: 14 January 2026 | **Revised:** 18 March 2026 | **Accepted:** 14 April 2026

Funding: Fundamental Research Funds for the Central Universities, Grant/Award Number: NE2025004

Keywords: metasurface antenna array | positive phase response | stable beam angle | wideband

ABSTRACT

A wideband positive phase response method is proposed and applied to the design of a series-fed dual-beam metasurface antenna (MSA) array. By employing two types of metasurface cells, two closely spaced resonant modes can be excited, thereby enabling a positive phase response over a wide frequency range for the MSA element. Then a dual-beam MSA array is realized by a two-port feeding network and four elements. Both simulated and measured results demonstrate that the proposed MSA array maintains a stable beam angle over a relative bandwidth of 20.4%. Compared with other designs in published literature, the proposed MSA array exhibits the advantages of a wideband stable beam angle, compact design, and simple structure. This demonstrates that the proposed positive phase response method is effective in achieving a wideband stable beam angle. Consequently, the MSA array developed using this approach shows strong potential for use in compact wideband wireless communication systems.

1 | Introduction

Given the limited availability of frequency spectrum resources, multi/dual-beam antennas with different beam coverages have received much attention by expanding space diversity ability [1]. In parallel-fed antenna arrays, fixed beam directions are typically achieved through the use of a beamforming network (BFN). In contrast, series-fed arrays commonly produce beam steering by adjusting the periodic spacing of the radiating elements. Compared with series-fed arrays, the parallel-fed array has the smaller frequency-scanning problem, while the series-fed array has a simpler structure. In [2], two BFNs were employed in a parallel-fed patch array to generate two independent beams directed at ±30°. However, such BFNs suffer from large physical footprints and non-negligible insertion losses, rendering them unsuitable for compact implementations. Series-fed antennas [3–6], on the other hand, can realize dual-beam radiation using compact and low-profile structures. For example, a dual-polarized single-layer series-fed patch array with high polarization purity was reported in [7], demonstrating the capability of series-fed structures for compact and efficient array implementations. In addition, millimeter-wave series-fed microstrip antenna arrays have also been investigated for high-gain and compact antenna systems [8]. Nevertheless, the beam direction of series-fed antennas typically varies with frequency due to the long-line effect, which is undesirable in applications requiring stable beam pointing. To mitigate the long-line effect, positive phase response methods have been introduced in series-fed array designs [9, 10]. Abnormal group delay phase shifters [9] were used in the transmission lines between e-lements to realize a positive phase response. As a consequence, the phase lag introduced by the long-line effect can be effectively counteracted. It should be noted that the core component of the abnormal phase shifter is a parallel RLC circuit. The bandwidth of a stable beam angle can be over 40%, but the insertion loss (2.47 dB) is unacceptable. Leaky-wave antenna arrays [4, 11] can provide wide-angle beam steering, but they generally suffer from severe frequency-scanning effects. A dual-polarized series-fed patch antenna array with two beams was reported in [12], yet its operating bandwidth is relatively narrow. Metasurface-based leaky-wave antennas were also developed in [13], offering compact structures but still experiencing beam variations across frequency. In [10], a narrow band of the stable beam was realized in a dual-beam ±45° dual-polarized series-fed metasurface antenna (MSA) array. It used the equivalent circuit of MSA to replace the phase shifter so that the large insertion loss can be avoided. However, the relative band of positive phase response is only 10% due to the single resonance of the MSA.

In this work, a stable dual-beam metasurface antenna array based on a wideband positive phase response is proposed. Inspired by [3, 10–17], a wider MSA element based on the dual parallel *RLC* equivalent circuit is designed. The MSA element employs two types of metasurface cells so that two nearby resonant modes are excited and a wideband positive phase response is realized. By using a two-port symmetric feeding network, one dual-beam MSA array with four elements is designed. Consequently, the beam angles of the proposed MSA array remain fixed and stable over a relative bandwidth of 20.4%. Compared with previously reported designs, the proposed MSA array exhibits a simpler configuration, broader operating bandwidth, and improved beam-angle stability.

2 | Analysis and Design of Stable-Beam Metasurface Antenna Array

This section presents a theoretical investigation of a wideband positive phase response mechanism tailored for series-fed arrays. Leveraging a dual-parallel RLC equivalent circuit model, this methodology is subsequently implemented in the design of the proposed MSA array to achieve enhanced performance.

2.1 | Theoretical Analysis of Stable-Beam Wideband Series-Fed Antenna Arrays

Considering the schematic of the series-fed antenna shown in Figure 1, multiple antenna elements are connected along a transmission line. The length and impedance of the transmission line are l and Z_i, respectively. To achieve the desired beam angle, the transmission-line length l can be calculated according to (1) in [10, 11].

$$4\pi l/\lambda_g = 2n\pi + 2\pi p_d \sin\theta_d/\lambda_0 \quad n = 1, 2, 3\ldots\ldots \tag{1}$$

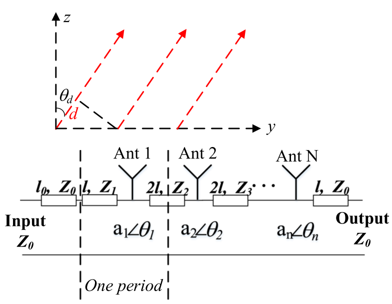

FIGURE 1 | Schematic of the series-fed antenna.

where λ_g is the guided wavelength, p_d is the period of antenna element, θ_d is the desired beam angle, λ_0 is the free-space wavelength, and n is an integer. Moreover, the impedance Z_i is optimized to achieve good matching and low side lobe level.

Take one period as an example, the phase response of the transmission line is negative and the phase response of the antenna zone is negative or ignored in the conventional series-fed design procedure. Consequently, the overall phase response of a single period is negative, which leads to frequency-scanning behavior in the array. To avoid this frequency-scanning problem and ensure the beam pointing to a fixed direction, it is necessary to control the phase response of one period in the series-fed array as desired over the working band.

Based on the above analysis, a method for implementing a positive phase response is proposed, as illustrated in Figure 2. The period can be divided into two transmission zones (phases 1 and 3) and one antenna zone (phase 2). As is well known, a parallel *RLC* circuit can generate a positive phase response around the resonant frequency [9, 10]. Considering the equivalent circuit of many antennas [10–12], the equivalent circuit can be simplified and represented by a parallel *RLC* circuit, where the *R* represents the radiation resistance and *LC* determines the resonate frequency. Under these circumstances, the antenna equivalent circuit can be utilized to generate a positive phase response, as illustrated in Figure 2a.

To further enhance the bandwidth of the positive phase response, a dual parallel RLC configuration is proposed, as shown in Figure 2b. When the parameters (C_1, L_1) and (C_2, L_2)

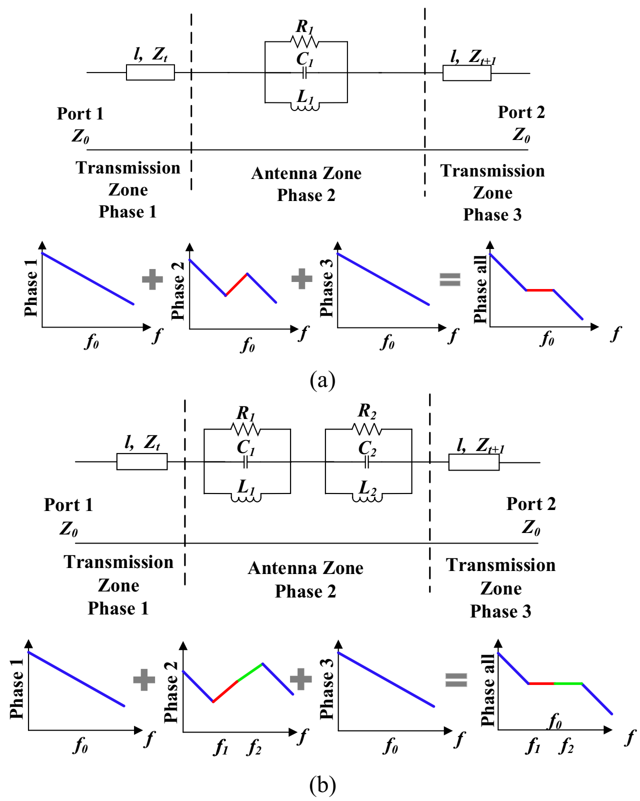

FIGURE 2 | Narrowband and wideband methods to overcome the frequency-scanning of the series-fed array. (a) Parallel *RLC* equivalent circuit of antenna element [8]. (b) Proposed dual parallel *RLC* equivalent circuit of the antenna element.

are selected appropriately and corresponding resonant frequencies f_1 and f_2 approach nearly the center frequency f_0, it is possible to generate a larger positive phase response band than the single parallel *RLC* circuit in [6]. This approach consequently enables a wideband stable beam angle. The next step is to realize the desired dual parallel RLC equivalent circuit through appropriate antenna element design.

2.2 | Realization of MSA Array With Wideband Stable Beam

As is well recognized, metasurface antenna elements are well suited for wideband antenna design owing to their inherent multimode resonance characteristics [15–17]. In this study, a dual-beam series-fed metasurface antenna array with a novel configuration is presented in Figure 3. The metasurface array consists of four metasurface antenna elements. Each MSA element consists of a 3 × 3 arrangement of metasurface cells excited by a two-port feeding network. Metasurface cells have two types of patches, one is the square patch and another is etched with a H-shaped slot. The H-shaped slots are etched into the patches with a one-row gap, and this configuration is used to excite two nearby resonant frequencies. Beneath the 3 × 3 metasurface cells, one coupling slot excited by a two-port microstrip line is etched into the metal ground. At the sides of the MSA array, four symmetric slots are etched in the metal ground to improve beam performance furtherly. The MSA elements are connected by the folded microstrip line to generate the radiated beam with the desired angle. The upper metasurface cells and lower feeding network are respectively constructed on substrate Rogers RO 4003 ($\varepsilon r = 3.55$, $\tan\delta = 0.0027$) and Rogers RT/duroid 5880 ($\varepsilon r = 2.2$, $\tan\delta = 0.0009$).

As shown in Figure 4, taking one MSA element as an example, it can be divided into three functional zones like Figure 2, which has two transmission zones on both sides and an antenna zone in the middle. In the transmission zone, the phase response (Phase 1 and 3) is negative against the frequency and its gradient is determined by the microstrip line length. However, the phase response (Phase 2) of the antenna zone would be positive, so that the negative Phase 1 and Phase 3 can be compensated. According to Figure 2b, the phase of MSA element can be adjusted if the equivalent circuit of the MSA element can be simplified by dual parallel *RLC*.

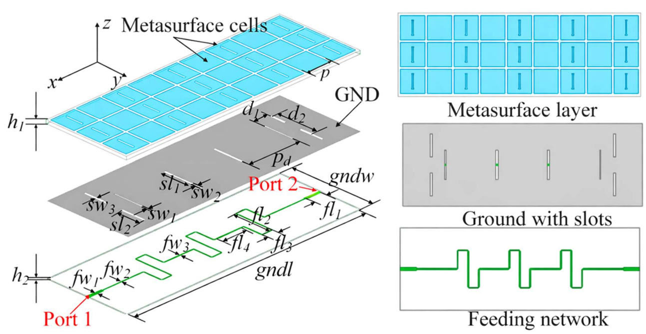

FIGURE 3 | Structure of the proposed MSA array. ($gndl = 109$ mm, $gndw = 37.5$ mm, $p = 12$ mm, $p_d = 23.5$ mm, $fl_1 = 9.25$ mm, $fl_2 = 16.9$ mm, $fl_3 = 4.75$ mm, $fl_4 = 13.5$ mm, $fw_1 = 1.46$ mm, $fw_2 = 0.5$ mm, $fw_3 = 0.7$ mm, $sl_1 = 13$ mm, $sl_2 = 10.5$ mm, $sw_1 = 0.25$ mm, $sw_2 = 1$ mm, $h_1 = 2$ mm, $h_2 = 0.5$ mm, $d_1 = 7$ mm, $d_2 = 17.5$ mm, $sl_2 = 10.5$ mm, $sw_3 = 1$ mm).

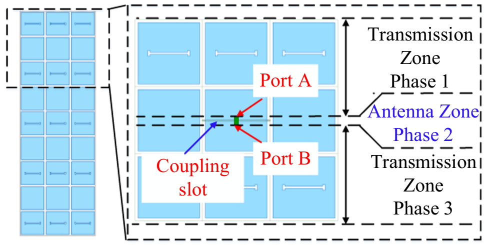

FIGURE 4 | Functional zones of MSA element.

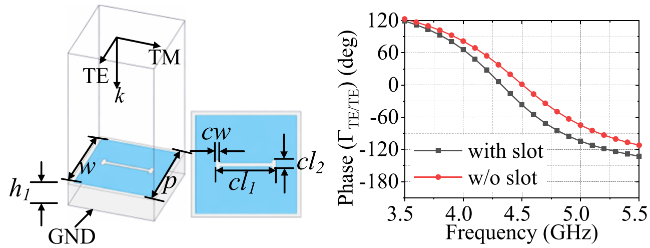

FIGURE 5 | Reflection phase of two types of metasurface cells. ($cw = 0.4$ mm, $cl_1 = 7.5$ mm, $cl_2 = 1$ mm, $w = 11$ mm, $h_1 = 2$ mm).

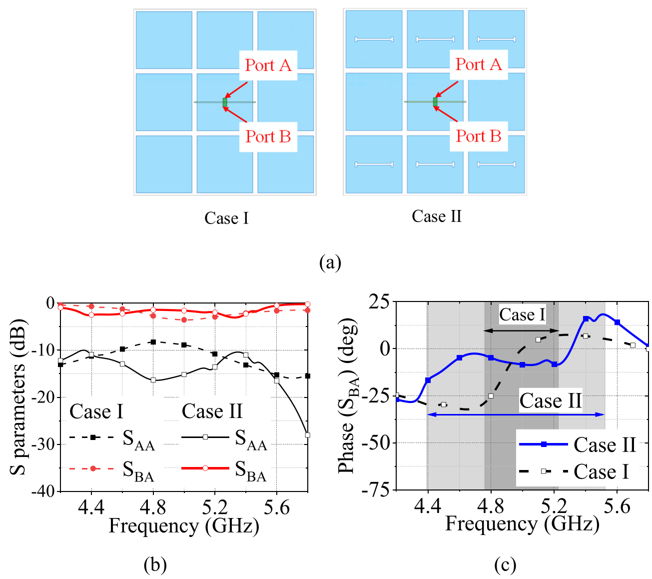

FIGURE 6 | (a) Case I: uniform metasurface cell, Case II: mixed metasurface cell. (b) S parameters of two Cases. (c) Phase response (S_{BA}) of two Cases to simulate Phase 2 in Figure 2.

To create the dual-resonance characteristic, two types of metasurface cells are employed in the antenna design. As shown in Figure 5, the reflection phases of metasurface cells are investigated by the Floquet-port model. The in-phase band (from −90° to 90°) of the metasurface cell with the H-shaped slot is a little lower than the in-phase band of the normal metasurface cell, indicating the resonant frequency of the metasurface cell with the slot is lower.

The positive phase responses of two cases are compared to illustrate the band improvement of the proposed MSA element. Case I uses square metasurface cells, while Case II employs mixed metasurface cells, as illustrated in Figure 6a. As shown in

Figure 6a–c, the S_{21} of Case II has two resonant frequencies around 5.0 GHz, while the S_{21} of Case I only has one resonant frequency. Moreover, the Phase (S_{BA}) of Case II has two stages of positive phase response from 4.3 to 5.5 GHz. However, the Phase (S_{BA}) of Case I has only one stage of positive phase response from 4.7 GHz to 5.3 GHz. These S-parameters performances verify the equivalent circuit of the proposed MSA element (Case II) can be simplified by dual parallel RLC in Figure 2b. Besides, the magnitude and phase of S_{BA} can be controlled by adjusting the sizes of coupling slots, MSA cells, and feeding networks [10, 11].

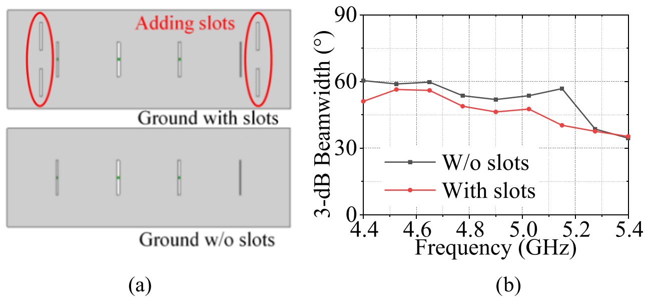

FIGURE 7 | MSA array with improved ground. (a) Metal ground with slots. (b) 3-dB beamwidth in xoz plane.

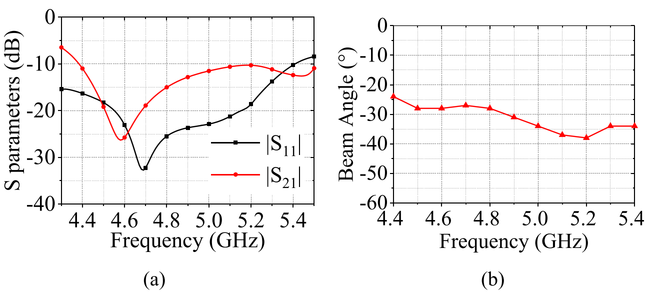

FIGURE 8 | (a) S parameters of MSA array. (b) Beam angle of MSA array.

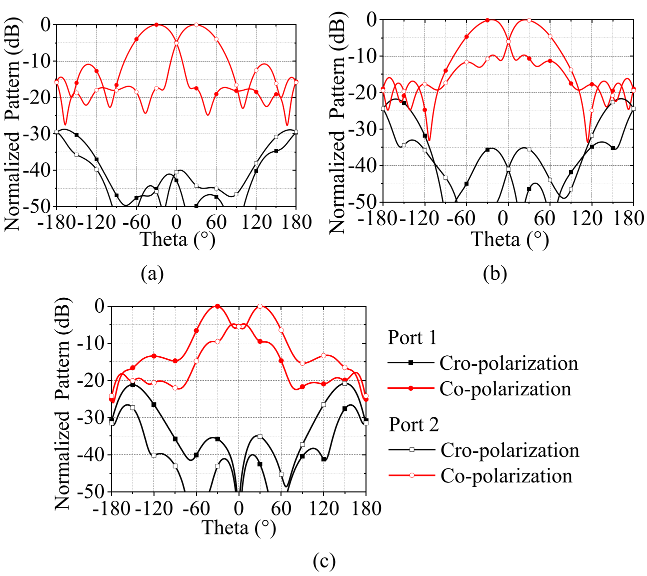

FIGURE 9 | Normalized radiation pattern. (a) 4.4 GHz. (b) 4.9 GHz. (c) 5.4 GHz.

Building upon the validated wideband positive phase response, a four-element series-fed MSA array was proposed, as illustrated in the schematic of Figure 3. The elements are series-fed and connected with a two-port folded microstrip line. Figure 7 shows the slots etched in the ground can reduce the beamwidth of the lower band, resulting in smaller beamwidth variation over the band of interest.

As shown in Figure 8, for the MSA array using the Case II element, the −10-dB impedance bandwidth is from 4.4 to 5.4 GHz, where the isolation is kept below −10 dB. The corresponding beam angle over the band is illustrated in Figure 8b. From 4.4 to 5.4 GHz, the beam angle ranges from −24° to −37° with a fluctuation of 13°. The detailed normalized radiation patterns within the band are illustrated in Figure 9. The beam angles are stable and the beams feature good space diversity. These results confirm that the designed MSA array, when im-

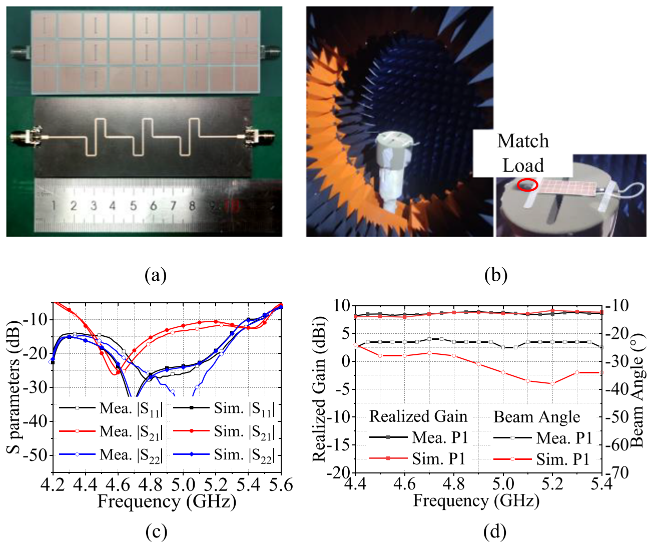

FIGURE 10 | (a) Front view of the fabricated prototype of the MSA array. (b) Measurement environment. (c) Measured and simulated S-parameters. (d) Gain and beam angle.

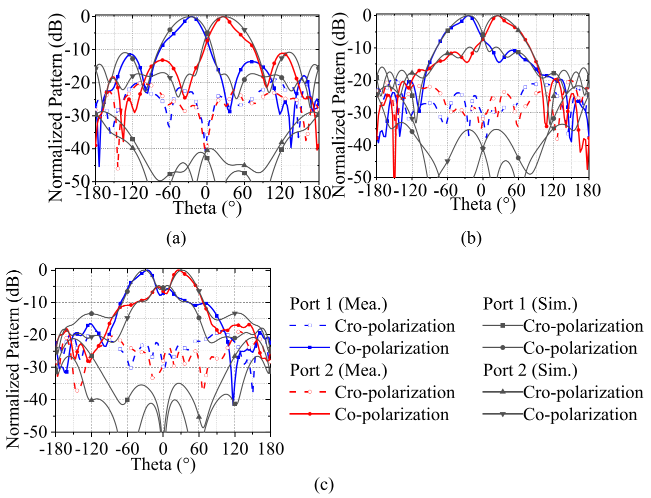

FIGURE 11 | Normalized radiation pattern of the dual-beam MSA array. (a) 4.4 GHz. (b) 4.9 GHz. (c) 5.4 GHz.

TABLE 1 | Comparison with Previously Reported Antennas.

Antenna type	Band (GHz)	Size (λ_0^3)	Polarization/Number of beams	Range of beam (deg)/R*	Peak gain (dBi)
Leaky-wave antenna array [4]	6.25–8.69 (32.7%)	$6.95 \times 1.36 \times 0.02$	Single polarization Single beam	18–76/177.4	16
SIW leaky-wave H-slot array [13]	10.1–11.9 (16.4%)	$11.4 \times 1.83 \times 0.04$	Single polarization Single beam	15–75/365.8	13.5
Series-fed patch array [3]	2.7–3.0 (10.5%)	$6.65 \times 0.67 \times 0.09$	Dual polarizations Two beams	20–30/95.2	
Leaky-wave array using metasurface [14]	9.5–10.45 (9.5%)	$4.4 \times 1.5 \times 0.8$	Single polarization Single beam	14–26/126	6.5
Series-fed MSA array [10]	4.9–5.5 (11.6%)	$2.5 \times 0.75 \times 0.05$	±45° dual polarizations Two beams	23.5–30/56.0	10.5
Series-fed MSA array [18]	5.25–5.55 (5.6%)	$1.85 \times 1.3 \times 0.06$	single polarization Two beams	24–30/107.1	12.3
Parallel-fed patch antenna array using wideband BFNs [19]	1.71–2.17 (23%)	$6.0 \times 2.27 \times 0.13$	±45° dual polarizations Two beams	20–31/47.8	16.4
This work	**4.4–5.4 (20.4%)**	$\mathbf{1.77 \times 0.625 \times 0.04}$	**Single polarization Two beams**	**Sim. 24–37/63.4 Mea. 19–25/29.3**	**9.8**

*R is ratio of beam variation to relative bandwidth.

plemented with this approach, achieves stable beam-angle performance over a wide operating bandwidth.

3 | Results and Discussions of MSA Array With Wideband Stable Beam

To experimentally validate the proposed design strategy for wideband positive phase response, a prototype of the MSA array was fabricated, as shown in Figure 10a. The S parameters were measured by a vector network analyzer (VNA), and the corresponding results are illustrated in Figure 10c. Good agreement between simulation and measurement is observed. Considering the band from 4.4 and 5.4 GHz, the S_{11} and S_{21} are both below -10dB. Radiation performances were measured by a Satimo Starlab near-field measurement system, which is shown in Figure 10b,d. The measured gain matches the simulated gain well, ranging from 8.2 dBi to 9.1 dBi. The measured beam angle changes from −19° to −25° with a fluctuation of 6°, which is better and more stable than the simulation results. Figure 11 shows the normalized radiation patterns at 4.4, 4.9, and 5.4 GHz have similar beam angles and the cross-polarization levels are kept below −20 dB. The measured main beams are slightly asymmetric and the beam angle fluctuation is smaller, which may be caused by the microwave chamber environment.

A performance comparison between the proposed array and previously reported works is summarized in Table 1. Series-fed leaky-wave antenna arrays [3, 4, 13, 14] can realize steerable beams, but they all suffer from the frequency-scanning problem. A narrow stable dual-beam MSA was realized in [8], in which the bandwidth is only about 11.6%. Compared with these arrays, a simpler stable dual-beam MSA array with wider bandwidth of 20.4% is observed in our work. Besides, the higher gain and narrower beamwidth can be achieved by further expanding the scale of MSA elements.

4 | Conclusion

This work presents an effective approach for wideband positive phase response control, which has been successfully applied to the design of an MSA array. By using the mixed MSA elements based on the dual parallel *RLC* equivalent circuit, a wideband positive phase response of element can be realized, so that the series-fed drawback of frequency scanning can be solved. As a result, a stable dual-beam MSA array is developed by adopting this design approach. Within the relative bandwidth of 20.4%, the beam angles are fixed and stable. The simulation and measurement results agree well, verifying the validity of the proposed design method. Compared to existing literature, the designed prototype has the advantages of a simpler structure, wider bandwidth, and more stable beam angle. These advantages indicate that the developed MSA array exhibits strong potential for use in compact dual-beam wireless communication systems.

Data Availability Statement

The data that support the findings of this study are available from the corresponding author upon reasonable request.

References

1. Y. Pan, Y. Cui, and R. Li, "Investigation of a Triple-Band Multibeam MIMO Antenna for Wireless Access Points," *IEEE Transactions on Antennas and Propagation* 64, no. 4 (2016): 1234–1241.

2. X. Y. Zhang, D. Xue, L. H. Ye, Y.-M. Pan, and Y. Zhang, "Compact Dual-Band Dual-Polarized Interleaved Two-Beam Array With Stable Radiation Pattern Based on Filtering Elements," *IEEE Transactions on Antennas and Propagation* 65, no. 9 (2017): 4566–4575.

3. S. Karimkashi and G. Zhang, "A Dual-Polarized Series-Fed Microstrip Antenna Array With Very High Polarization Purity for Weather Measurements," *IEEE Transactions on Antennas and Propagation* 61, no. 10 (2013): 5315–5319.

4. J. Liu, Y. Li, and Y. Long, "Design of Periodic Shorting-Vias for Suppressing the Fundamental Mode in Microstrip Leaky-Wave Antennas," *IEEE Transactions on Antennas and Propagation* 63, no. 10 (2015): 4297–4304.

5. Q. Zhang, Q. Zhang, H. Liu, and C. H. Chan, "Dual-Band and Dual-Polarized Leaky-Wave Antenna Based on Slotted Siw," *IEEE Antennas and Wireless Propagation Letters* 18, no. 3 (2019): 507–511.

6. D. J. Wei, J. Li, J. Liu, G. Yang, and W. Zhang, "Dual-Band Substrate-Integrated Waveguide Leaky-Wave Antenna With a Simple Feeding Way," *IEEE Antennas and Wireless Propagation Letters* 18, no. 4 (2019): 591–595.

7. S. Keser and M. Mojahedi, "Removal of Beam Squint in Series Fed Array Antennas Using Abnormal Group Delay Phase Shifters," in *2010 IEEE Antennas and Propagation Society International Symposium* (2010), 1–4.

8. C. Deng, B. Yektakhah, and K. Sarabandi, "Series-Fed Dual-Polarized Single-Layer Linear Patch Array With High Polarization Purity," *IEEE Antennas and Wireless Propagation Letters* 18, no. 9 (2019): 1746–1750.

9. S. David Joseph and E. A. Ball, "Series-Fed Millimeter-Wave Antenna Array Based on Microstrip Line Structure," *IEEE Open Journal of Antennas and Propagation* 4 (2023): 254–261.

10. L. Gu, W. Yang, Q. Xue, and W. Che, "A ±45° Dual-Polarized Dual-Beam Series-Fed Metasurface Antenna Array With Stable Beam Angle," *IEEE Transactions on Antennas and Propagation* 69, no. 12 (2021): 8366–8375.

11. L. Gu, W. Yang, Q. Xue, and W. Che, "A Dual-Band Steerable Dual-Beam Metasurface Antenna Based on Common Feeding Network," *IEEE Transactions on Antennas and Propagation* 69, no. 10 (2021): 6340–6350.

12. N. W. Liu, G. Fu, and L. Zhu, "Low-Profile Multi-Mode Wideband Patch Antennas," in *2018 Cross Strait Quad-Regional Radio Science and Wireless Technology Conference (CSQRWC)* (2018), 1–3.

13. J. Liu, X. Tang, Y. Li, and Y. Long, "Substrate Integrated Waveguide Leaky-Wave Antenna With H-Shaped Slots," *IEEE Transactions on Antennas and Propagation* 60, no. 8 (2012): 3962–3967.

14. X. Wan, T. Y. Chen, X. Q. Chen, L. Zhang, and T. J. Cui, "Beam Forming of Leaky Waves at Fixed Frequency Using Binary Programmable Metasurface," *IEEE Transactions on Antennas and Propagation* 66, no. 9 (2018): 4942–4947.

15. B. Cheng, Z. Du, and D. Huang, "A Differentially Fed Broadband Multimode Microstrip Antenna," *IEEE Antennas and Wireless Propagation Letters* 19, no. 5 (2020): 771–775.

16. B. Cheng, Z. Du, and D. Huang, "A Broadband Low-Profile Multimode Microstrip Antenna," *IEEE Antennas and Wireless Propagation Letters* 18, no. 7 (2019): 1332–1336.

17. J. Wu, Z. Huang, X. Ren, W. E. I. Sha, and X. Wu, "Wideband Millimeter-Wave Dual-Mode Dual Circularly Polarized OAM Antenna Using Sequentially Rotated Feeding Technique," *IEEE Antennas and Wireless Propagation Letters* 19, no. 8 (2020): 1296–1300.

18. W. Yang, L. Gu, W. Che, Q. Meng, Q. Xue, and C. Wan, "A Novel Steerable Dual-Beam Metasurface Antenna Based on Controllable Feeding Mechanism," *IEEE Transactions on Antennas and Propagation* 67, no. 2 (2019): 784–793.

19. X.-Y. Zhang, D. Xue, L.-H. Ye, Y.-M. Pan, and Y. Zhang, "Compact Dual-Band Dual-Polarized Interleaved Two-Beam Array With Stable Radiation Pattern Based on Filtering Elements," *IEEE Transactions on Antennas and Propagation* 65, no. 9 (2017): 4566–4575.